

Image Lightness Rescaling Using Sigmoidal Contrast Enhancement Functions

Gustav J. Braun and Mark D. Fairchild

Munsell Color Science Laboratory
Center for Imaging Science
Rochester Institute of Technology
Rochester, New York

ABSTRACT

In color gamut mapping of pictorial images, the lightness rendition of the mapped images plays a major role in the quality of the final image. For color gamut mapping tasks, where the goal is to produce a match to the original scene, it is important to maintain the perceived lightness contrast of the original image. Typical lightness remapping functions such as linear compression, soft compression, and hard clipping reduce the lightness contrast of the input image. Sigmoidal remapping functions were utilized to overcome the natural loss in perceived lightness contrast that results when an image from a full dynamic range device is scaled into the limited dynamic range of a destination device. These functions were tuned to the particular lightness characteristics of the images used and the selected dynamic ranges. The sigmoidal remapping functions were selected based on an empirical contrast enhancement model that was developed from the results of a psychophysical adjustment experiment. The results of this study showed that it was possible to maintain the perceived lightness contrast of the images by using sigmoidal contrast enhancement functions to selectively rescale images from a source device with a full dynamic range into a destination device with a limited dynamic range.

Keywords: Gamut mapping, lightness rescaling, image processing, contrast enhancement

1. INTRODUCTION

One of the most important factors in a color gamut mapping process for pictorial images is that the final image maintains the lightness integrity of the original scene. Often times an output device, such as an inkjet or laser printer, does not possess the lightness dynamic range that is present in the original scene (e.g., that of a CRT or a glossy photographic original). When the large input dynamic range is rescaled to fit into the smaller output dynamic range, significant image contrast may be lost.

Various lightness-remapping schemes have been formulated to account for these dynamic range differences. Linear lightness rescaling is one commonly used process^{1,2}. In this case, source pixel lightness values are processed through the following linear scaling equation:

$$L_{out}^* = \frac{L_{in}^*}{100} (100 - L_{minOut}^*) + L_{minOut}^* , \quad (1)$$

where L_{out}^* , L_{in}^* , and L_{minOut}^* are the mapped lightness, the lightnesses of the source pixels, and the minimum lightness of the destination device respectively. In general, the source pixels will not have lightnesses that span the entire CIELAB L^* {0,100} range. As such, a slight modification can be made to the remapping function given in Equation 1 where the range of input *data* is scaled into the range of the destination device¹. Thus, the source pixel data are first normalized to a full lightness range (i.e., $\{L_{minIn}^*, 100\} \rightarrow \{0, 1\}$) then rescaled into the full range of the destination device (i.e., $\{L_{minOut}^*, 100\}$) as shown in Equation 2.

$$L_{out}^* = \frac{L_{in}^* - L_{minIn}^*}{100 - L_{minIn}^*} (100 - L_{minOut}^*) + L_{minOut}^* , \quad (2)$$

When the L_{minIn}^* value is significantly greater than zero, this process more efficiently utilizes the limited dynamic range of the output medium. In spite of this modification, the linear lightness remapping process suffers from a global reduction in the perceived lightness contrast and an increase in the mean lightness of the remapped image. When the dynamic range difference between the source and destination devices is significant, output images tend to appear light and often times contain a “milky” appearance in the shadow detail.

Lightness clipping algorithms (“hard clipping”) can be applied to reduce the loss in perceived lightness contrast obtained when the destination dynamic range is less than the source dynamic range. In this case, all of the source pixel lightnesses that are less than the destination device’s black point lightness are clipped to that black point lightness. In general, this process can *approximately* maintain the mean lightness of the image. The major shortcoming of this process is the potential for significant loss in image texture resulting from the many-to-one mapping. For images that contain significant amounts of shadow detail below the $L^*_{\min\text{Out}}$ lightness, clipping results in a “flattening” of the shadowed regions. This phenomenon is accentuated as the $L^*_{\min\text{Out}}$ increases.

In an effort to overcome the loss in detail associated with “hard clipping”, “soft clipping” procedures have been applied^{1,3}. Examples of some typical soft clipping functions are given in Figure 1. These functions can be broken down into two regions. In the first region, the contrast is compressed in the shadow detail unlike straight clipping. In the second region, an identity mapping is utilized, $L^*_{\text{out}} = L^*_{\text{in}}$. As a result, the lightness contrast in the shadow region is compressed but the texture remains visible. The two forms of the soft-clipping functions shown in Figure 1 are knee compression and soft compression. The soft compression function increases the rate of compression as the minimum lightness is approached. The knee function applies the same compression rate throughout the compression region (piece-wise linear).

While, soft and knee compression rescalings offer more flexibility than hard clipping or linear lightness rescaling, it is difficult to generalize these processes for all image types and dynamic ranges. As the black point of the destination device increases progressively to higher lightnesses, progressively more low-end compression is needed. The ways to achieve this are by: 1.) Making the knee segment or the soft compression region more severe or 2.) utilizing a smaller linear remapping region. Each of these options will reduce the perceived lightness contrast of the remapped images.

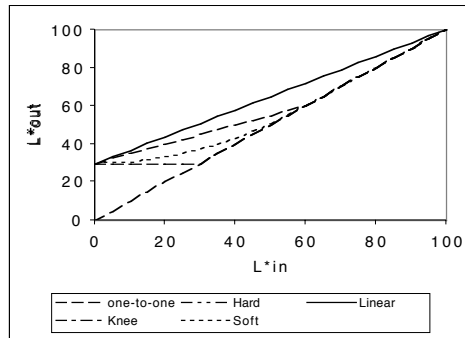


Figure 1. An illustration of various lightness rescaling processes. Linear compression follows that given in Equation 1. The hard clipping example sets all input L^* values less than 30 to an output of $L^*=30$. The knee compression function performs linear compression of input L^* values from $\{0, 60\}$ into the output range of $\{30, 60\}$. The soft compression function gradually compresses the input L^* values between $\{0, 60\}$ into the output range of $\{30, 60\}$.

2. SIGMOIDAL LIGHTNESS RESCALING FUNCTIONS

The biggest limitation with the lightness remapping strategies previously discussed is that they fail to universally address the fact that as the dynamic range decreases the perceived contrast of the image decreases. As such, it is desirable to develop a remapping strategy that will perform the range compression while maintaining the perceived image contrast. The proposed solution to this problem was to develop a function that would be tunable such that as the dynamic range decreased, the function would boost the image contrast accordingly. In order to boost the image contrast in the limited dynamic range, both the highlight and the shadow detail need to be compressed. This was accomplished by utilizing a sigmoidal remapping function. The form of the sigmoidal functions was derived from a discrete cumulative normal function (S), given in Equation 3, where x_0 and σ are the mean and variance of the normal distribution respectively, $i = 0, 1, 2 \dots m$, and m is the number of points used in the discrete look-up table.

$$s_i = \sum_{n=0}^{n=i} \frac{1}{\sqrt{2\pi\sigma}} e^{-\frac{(x_n - x_0)^2}{2\sigma^2}}, \quad (3)$$

The x_0 and σ parameters control the shape of the sigmoids. The value of x_0 controls the centering of the sigmoid and σ controls the slope. Making x_0 greater than $L^*=50$ shifts the straight-line portion of the sigmoid toward higher lightnesses. An x_0 value of less than $L^*=50$ shifts the straight-line portion of the sigmoid toward the lower lightnesses. These relationships are shown in Figure 2a where $\sigma=15$. In a similar manner, a family of sigmoidal remapping curves can be generated by holding the x_0 parameter fixed, at $L^*=50$ for example, and varying the σ parameter, Figure 2b. Decreasing the σ value has the effect of increasing the contrast of the remapped image. Shifting the distribution toward lower lightnesses (i.e., decreasing x_0) has the effect of applying more highlight compression, while shifting the distribution toward higher lightnesses (i.e., increasing x_0) results in more shadow compression. By adjusting x_0 and σ it is possible to tailor a remapping function with an appropriate amount of image contrast enhancement and highlight and shadow lightness compression.

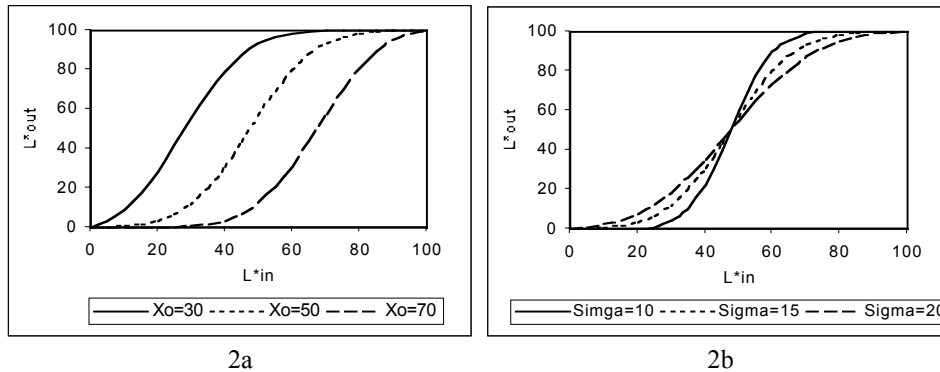


Figure 2. a.) Family of sigmoidal contrast enhancement functions that have equal σ parameters and varying x_0 parameters. As the x_0 parameter increases there is more compression of the shadow detail than the highlight detail b.) Family of sigmoidal contrast enhancement functions that have equal x_0 parameters and varying σ parameters. As the σ parameter is decreased the remapping function increases the image contrast by boosting the slope in the mid-tones while equally compressing the highlight and the shadow detail.

3. SIMULTANEOUS LIGHTNESS CONTRAST

The hypothesis of using sigmoidal functions for lightness remapping is based on the phenomenon of simultaneous lightness contrast. It is possible to make the dark colors in an image look darker by making the light colors lighter. This is accomplished using the sigmoidal functions. As σ decreases the effect is to lighten the highlights and darken the shadowed regions. As the lightness difference between the highlight and shadow regions increases, the image contrast increases giving the appearance of a larger dynamic range. By adjusting x_0 and σ together, it is possible to tailor the amount of lightening and darkening of the highlight and shadowed regions to control the overall contrast enhancement.

4. EXPERIMENTAL

4.1 Phase 1 - Visual optimization of x_0 and σ : User adjustments

Typical pictorial images contain a range of shadow and highlight detail depending on the composition of the scene portrayed in the image. Information regarding the lightness composition of the image can be obtained from its lightness histogram. For the purposes of this study, lightness histograms were broken down into four categories: low lightness key (skewed toward low lightness), high lightness key (skewed toward high lightness), normal lightness key (“Gaussian” shaped histogram), and uniform lightness key (“flat” histogram over most of the lightness range). It was theorized that the form of the sigmoidal lightness remapping function would depend on the lightness composition of the image (i.e., its lightness histogram) as well as the dynamic range difference between the source and the destination devices. MacAdam⁴ showed that different sigmoidal density tone transfer curves were required for optimal reproduction of images that had predominantly shadow or highlight features.

Based on these observations, a psychophysical experiment was conducted to determine optimal sigmoidal contrast enhancement functions for images from each of the lightness keys mentioned above, at four destination dynamic ranges ($L^*_{\min\text{Out}} = \{5, 10, 15, 20\}$). This experiment consisted of user adjustments that were performed on six CRT images that were

selected based on their lightness histograms (Figure 4a-f). These included, 1 high lightness-key image, 1 low lightness-key image, 2 normal lightness-key images, and 2 uniform lightness-key images (Figure 3a-f). (Note: Lightness images were

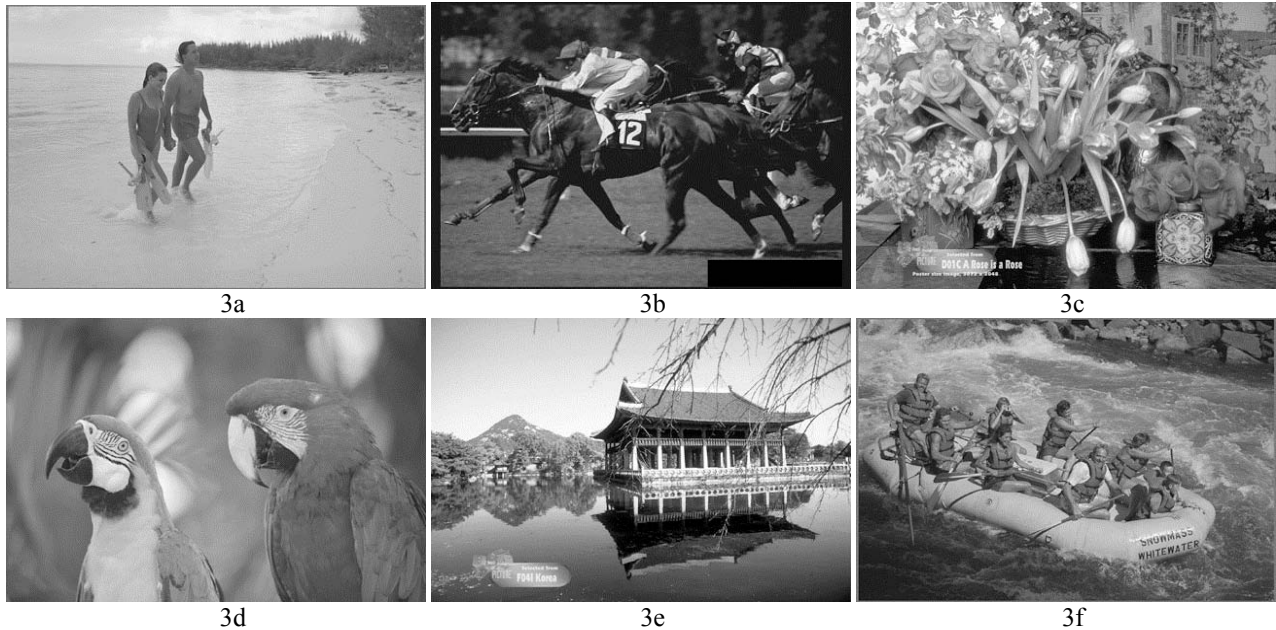


Figure 3a-f. Lightness images for the six test images used in the user adjustment experiments; a.) “Couple-On-Beach”; b.) “Horse-Race”; c.) “Flowers”; d.) “Macaws”; e.) “Temple”; f.) “Raft”.

generated using the gain-offset-gamma characteristics of the Sony GDM-2000TC monitor to convert from device digital counts to CIELAB L^* , according to the model established by Berns, Motta, and Gorzynski.⁵) The adjustments consisted of having users interactively control the shapes of the sigmoidal lightness (CIELAB L^*) remapping functions. In this experiment, only the calibrated grayscale lightness channel was presented to the observers for each image. This made it

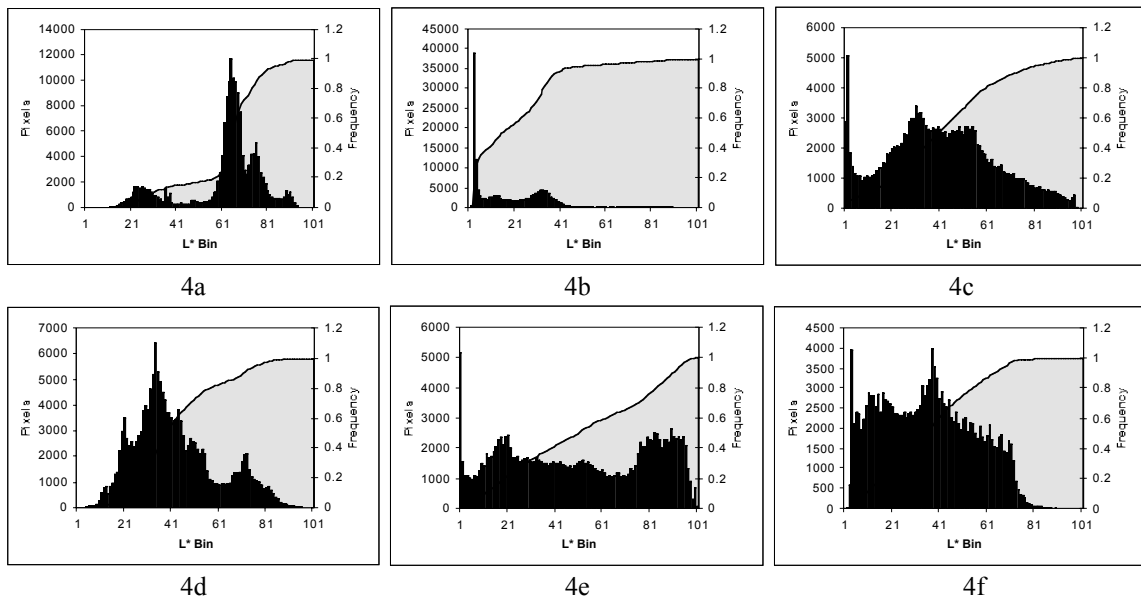


Figure 4a-f. Lightness histograms (bars) and cumulative lightness histograms (solid gray patches) for the six reference images; a.) “Couple-On-Beach”; b.) “Horse-Race”; c.) “Flowers”; d.) “Macaws”; e.) “Temple”; f.) “Raft”.

possible for the observers to interactively remap the lightness image in real time. The premise behind adjusting only the lightness image was that the lightness information could be visually separated from the chromatic information. In addition, it

was hypothesized that the optimal lightness remappings that were obtained from the grayscale adjustments would be the same optimal lightness remappings when the chromatic content of the scene was added back in. (Note: This was confirmed in Phase 2 and Phase 3 where the chromatic content was added back.) For each observer, the adjustments resulted in optimal settings for the sigmoidal rescaling curves.

The user interface developed for this experiment is shown in Figure 5. Subjects controlled sliders that dynamically updated the values for x_0 and σ . In turn, the form of the sigmoidal remapping function was adjusted accordingly. The task presented to the subjects was to adjust the image in the right field (the reduced dynamic range condition) so that it matched the image in the left field (the original full dynamic range condition). For this experiment, adjustments were made for each of the six images at four different $L^*_{\min\text{Out}}$ levels ($L^*_{\min\text{Out}} = 5, 10, 15, \text{ and } 20$). In all, six subjects took part in the adjustment experiment. The subjects were experienced with these types of adjustments.



Figure 5. User interface for adjustment experiment. The subjects adjusted the x_0 and σ sliders until the reduced dynamic range image (right image) was the best possible match to the original full dynamic range image (left image).

The results of the observer adjustments are represented graphically in Figure 6a-f. Based on the large inter-observer variability obtained from these adjustments, an “average observer” response was generated from the numerical average of the individual adjustments. The solid trend lines shown in Figure 6a-f represent the average observer responses. Overall, as the minimum lightness of the destination device increased, the average-observer x_0 parameter increased and the average-observer σ decreased. This trend indicates that as the dynamic range decreased more compression was required in the low lightness region, as evidenced by the increase x_0 . Similarly, the trend lines for the σ parameter indicate that a contrast boost (decrease in σ) is required as the dynamic range decreases.

4.2 Phase 2 - Selection of candidate remapping curves

The user adjustment results shown in Figure 6a-f indicate a significant amount of inter-observer variability. As such, it was decided that the “average observer” curve should be used only as a *candidate* for the optimal x_0 and σ parameters. Therefore, for each of the six test images, a family of curves was generated for each $L^*_{\min\text{Out}}$ level. The x_0 and σ settings for these curves were determined based on the standard deviation of the inter-observer variability at each of the $L^*_{\min\text{Out}}$ adjustment levels. For example, for the "Macaws" image, at a minimum $L^*=10$, there were six estimates of x_0 (i.e., one from each observer). The mean of these x_0 settings made up one point in the “average observer” trend line for that image. Two other estimates were then made of x_0 by taking $x_0 \pm \sigma_{x_0}$, where σ_{x_0} was the standard deviation of the inter-observer variability for x_0 . The same process was used to generate three estimates of σ at each minimum L^* level for each image. Given the three estimates for x_0 and the three estimates for σ there were nine candidate contrast enhancement curves (S_1, S_2, \dots, S_9), at each minimum L^* level, for each of the six reference images (i.e., $S_1=f(x_0, \sigma)$, $S_2=f(x_0, \sigma+\sigma_{\sigma_0})$, $S_3=f(x_0, \sigma-\sigma_{\sigma_0})$, $S_4=f(x_0+\sigma_{x_0}, \sigma)$, $S_5=f(x_0+\sigma_{x_0}, \sigma+\sigma_{\sigma_0})$, $S_6=f(x_0+\sigma_{x_0}, \sigma-\sigma_{\sigma_0})$, $S_7=f(x_0-\sigma_{x_0}, \sigma)$, $S_8=f(x_0-\sigma_{x_0}, \sigma+\sigma_{\sigma_0})$, $S_9=f(x_0-\sigma_{x_0}, \sigma-\sigma_{\sigma_0})$).

In order to determine which of these nine candidate remapping functions produced the best match to an original image for a given destination $L^*_{\min\text{Out}}$, a psychophysical test was performed. Thus, for each image, 36 lightness-compressed images were generated (i.e., 4 minimum L^* levels times 9 candidate sigmoids per level). Since the ultimate goal of this research was to apply the sigmoidal lightness compression on color images, the lightness compressed images were recombined with their corresponding hue and chroma data (i.e., CIELAB h_{ab} and C^*_{ab} respectively). Thus, the remapped

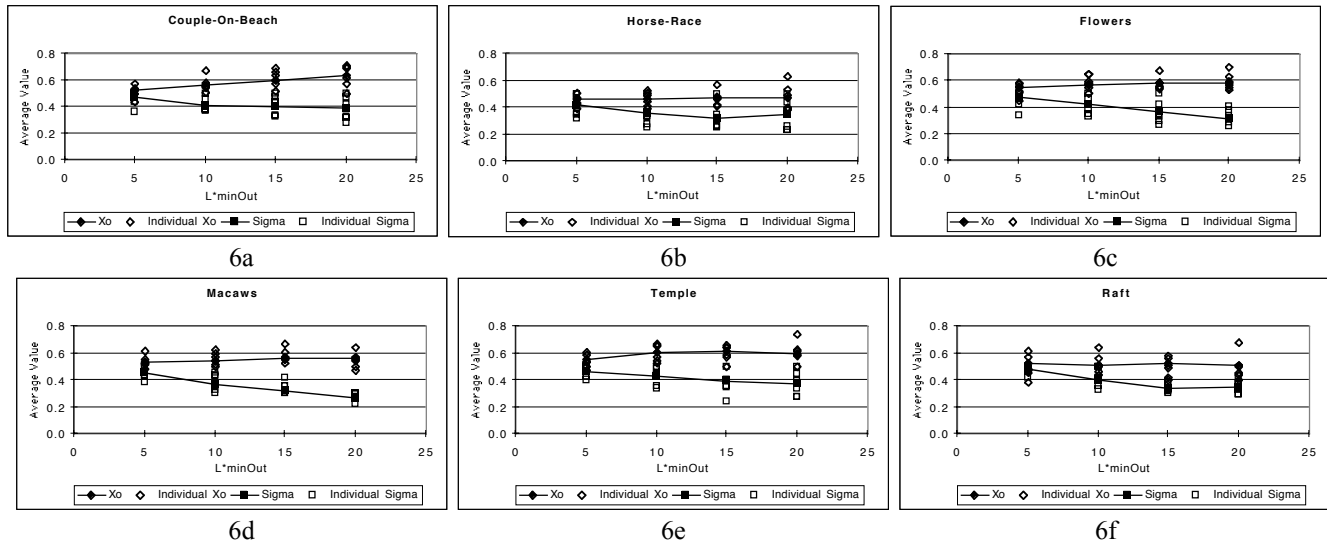


Figure 6a-f. Sigmoidal parameter curves from the adjustment experiment. These plots give the x_0 and σ settings that each of the six subjects determined produced a visual match, to the original full dynamic range image, under the four reduced dynamic range conditions. The solid lines in each plot represent the trend lines that connect the average x_0 and σ parameters taken from the individual subject responses ((open squares) represent the x_0 responses, (open diamonds) represent the σ responses).

images were identical in hue and essentially identical in chroma to the original. (Note: The lightness remapping of a pixel may have moved that pixel's color out-of-gamut. As a result, after the lightness remapping, all pixels that were out-of-gamut were chroma clipped to the surface of the gamut while preserving lightness and hue angle. These mappings were performed in the Hung and Berns hue-linearized CIELAB color space⁶.)

A screening experiment was then performed on the full-color images to eliminate the obviously poor performing remapping functions. Only one observer performed this task since for six images, with four minimum L^* levels per image, and nine sigmoid settings per level, the number of pairs exceeded 800. This was far too many image pair comparisons for multiple subjects. The one subject that performed this task was experienced in these types of observations. Since there was only one observation per image, the paired comparison data could not be analyzed using Thurstone's law of Comparative Judgements⁷. As such, the results of these observations were analyzed by tallying the number of times a given setting was selected as the best. Thus, at each $L^*_{\min\text{Out}}$ setting, for each image, there was a histogram of number of times a given setting (S_1 - S_9) was selected as a better match. For example, for the "Temple" image at $L^*_{\min\text{Out}}=10$, there were nine images mapped through their corresponding S_1 - S_9 sigmoidal remapping functions. These images were compared in pairs to the original. Each remapped image was compared to the eight other remapped images at that $L^*_{\min\text{Out}}$ value. A tally was taken of the number of times a given image was selected as the better match to the original. The tallied data from these observations are given in Table 1 (Appendix).

4.3 Phase 3 - Selection of optimal rescaling curves

The highlighted images in Table 1 advanced into the third visual experiment. These final candidate images were shown, in pairs, to 21 observers. Their task was to select the image that was the closest match to the original scene. The results of this experiment were 24 interval scales⁷ (i.e., one for each of the four minimum L^* levels, for each of the six images) that were used to select an optimal pair of x_0 and σ values. The interval scales are shown in Table 2 (Appendix). The x_0 and σ values associated with the highlighted settings were selected as the optimal sigmoid parameters for the different images and $L^*_{\min\text{Out}}$ levels. In general, the optimized parameters followed the same trends as with the average-observer curves: as the $L^*_{\min\text{Out}}$ increased the amount of contrast boosting increased.

For some of the images there were dips present in the x_0 and σ parameter curves. For example, in the "Couple-on-Beach" image the x_0 and σ values for the minimum $L^*=15$ level were significantly lower than for any of the other settings, Figure 7. The x_0 and σ values at minimum $L^*=15$ were not in line with the values at the other $L^*_{\min\text{Out}}$ settings. As such, the x_0 and σ parameters for this level were increased until they fell naturally in line with the other settings for this image. Intuitively there

should not be discontinuities in the remapping curves between minimum L^* levels of 10 and 15, or of 15 and 20 within an image. The reason for this was that the scene content did not change; only the output dynamic range changed.

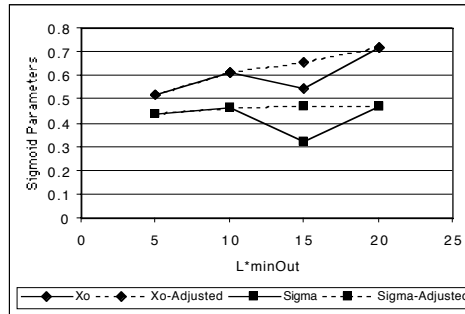


Figure 7. The solid lines represent the x_0 and σ parameters resulting from the Phase 3 visual experiment. The “dip” in the estimated parameters for the $L^*_{\min Out}=15$ setting was adjusted so that it fell in line with the settings at the other $L^*_{\min Out}$ levels (dashed lines).

Similar adjustments were made to the parameter curves for the "Macaws", "Raft", and "Temple" images. Upon visual inspection, these adjustments produced images that were equal, if not superior, in quality to the unadjusted curves. The final forms of the "optimal" sigmoid parameter curves are given in Figures 8a-c. These curves have been grouped together based on their similarity.

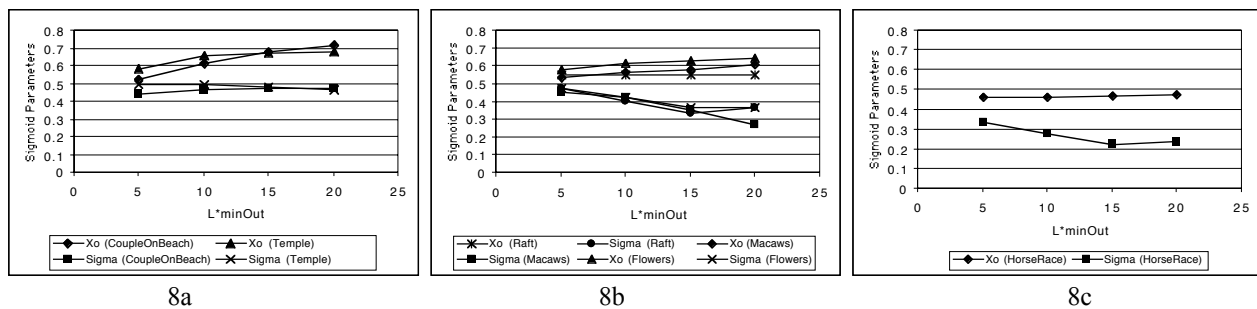


Figure 8a-c. Optimal x_0 and σ parameters as a function of $L^*_{\min Out}$ for the test images sorted into the three image lightness-classes. a.) The sigmoid parameters for the high lightness-class images (“Couple-On-Beach” and “Temple”). b.) The sigmoid parameters for the normal lightness-class images (“Flowers”, “Raft”, and “Macaws”). c.) The sigmoid parameters for the low lightness-class image (“Horse-Race”).

5. ANALYSIS OF PHASE 3 X_0 AND σ PARAMETER CURVES

5.1 Image groupings

Analysis of the form of the x_0 and σ parameter curves for the six images revealed that there was considerable correlation between several images (Figure 8). Originally the images were classified into four groups; low lightness-key, high lightness-key, normal lightness-key, and uniform lightness-key. The results of this experiment tend to indicate that, of the images tested, three lightness-classes were enough to categorize the images; these classes were high lightness class, normal lightness class, and low lightness class. As such, the “Couple-On-Beach” image and the “Temple” were grouped together into the high lightness-class because their corresponding x_0 and σ parameter curves were nearly identical. The new normal lightness-class consisted of the “Flowers”, “Macaws”, and “Raft” images. The low lightness-class consisted only of the “Horse-Race” image since it was considerably different than any of the other images.

5.2 Analysis of the lightness-class groupings

For the high lightness-class, the “Couple-On-Beach” and “Temple” images resulted in nearly identical x_0 and σ parameter curves because they both had a significant amount of highlight information. This was revealed by examining the cumulative lightness histograms for these images (Figure 4a, 4e). For these images, the 75 percent points of their cumulative lightness histograms occurred at lightness values of greater than 70. The sigmoidal remapping functions used in this study compress

both the highlight and shadowed regions to increase the perceived image contrast (i.e., simultaneous lightness contrast). Essentially, the shadowed regions are made to appear darker by compressing them while simultaneously lightening the highlight regions. Since these images contained proportionately the same amount of highlight regions, the same x_0 and σ parameter curves performed well for them.

Similar trends in the x_0 and σ parameter curves were noticed for the three images that were grouped into the normal lightness-class ("Flowers", "Macaws", and "Raft"), Figure 8b. The 75 percent points of their cumulative lightness histograms occurred at 55, 51, and 50 lightness units for the "Flowers", "Macaws", and "Raft" images respectively (Figures 4c,d,f). These three images had nearly identical σ curves and had x_0 curves that looked like shifted copies of each other. The similarity in the proportionate amounts of highlight and shadow detail point to the similarity in the x_0 and σ curves for these images.

Finally, in the low lightness-class category, the "Horse-Race" image had the least amount of highlight detail and the most amount of shadow detail. This was indicated by its rapidly rising cumulative lightness histogram shown in Figure 4b. The corresponding 75 percent point of its cumulative lightness histogram occurred at $L^*=31$. Thus, 75 percent of the entire image pixels occur in essentially one third of the entire lightness dynamic range. In this case the x_0 and σ parameter curves apply more highlight compression than shadow compression.

5.3 Curve consolidations

The parameter curves were grouped together into three distinct lightness-classes in an effort to consolidate the individual image x_0 and σ parameter curves into a single parameter curve that described these parameters for the entire class. Based on the high correlation between the x_0 and σ parameter curves in the high lightness-class (Figure 8a) it was possible to use the x_0 and σ parameter curves for the "Couple-on-Beach" image to predict the contrast enhancement needed for the "Temple" image. When this was done, there were no significant changes noticed in the appearance of the mapped "Temple" image. The plot shown in Figure 9a gives the final form of the high lightness-class x_0 and σ parameter curves.

Similar correlation was found between the normal lightness-key images, "Macaws" and "Flowers", and the uniform lightness-key "Raft" image, Figure 8b. The σ curves for these three images were nearly identical. The exception was for high minimum L^* settings. In this case the σ curve for the "Macaws" image had an essentially linear, decreasing, relationship as a function of minimum L^* . The σ curves for the other two images were essentially linear from minimum $L^*=5$ to 15 and then leveled out for minimum $L^*=20$. The reason for this was that there was slightly more information in the "Flowers" and "Raft" images at lower lightness values. Since the amount of low-end compression increased with $L^*_{\min\text{Out}}$, the contrast boost associated with decreasing σ and increasing x_0 needed to level off for the "Raft" and "Flowers" images. This helped to insure that the low-end shadow detail did not get compressed to the point where all of the lightness contrast was eliminated. Based on the high correlation that existed for the σ parameter curves, a composite σ curve was generated for the normal lightness-class. This curve followed a nearly linear decrease in σ up to $L^*_{\min\text{Out}}=15$ and then flattened out to a value at $L^*_{\min\text{Out}}=20$ of the average of the parameters from the three normal lightness-key images, Figure 9b.

The systematic differences between the x_0 curves for the three images (Figure 8b) in the normal lightness-class made it difficult to consolidate them into a single x_0 parameter curve for the class. A ranking of these curves (e.g., highest, middle, and lowest) compared directly with the lightness of the 75 percent point of their respective cumulative lightness histograms. The rankings of the x_0 curves was highest="Flowers", middle="Macaws", lowest="Raft". The lightness values for the 75 percent point of the images cumulative lightness histograms were 55, 51, and 50 for the "Flowers", "Macaws", and "Raft" images respectively. The x_0 parameter curves for the normal lightness-key images "blended" very smoothly between the shape of the x_0 curves for the low lightness-class and the high lightness-class. The "Raft" image had an x_0 curve that was similar to that of the low lightness-class. The 75 percent point of the "Raft" image was the closest to the "Horse-Race" image for all of the images in normal lightness-class. The x_0 curve for the "Flowers" image was similar in shape and magnitude to the high lightness-class. The value of the 75 percent point for this image was the highest of the images in the normal lightness-class. The "Macaws" image fell in between the "Raft" and the "Flowers" image in both x_0 curve shape and 75 percent point of the cumulative lightness histograms. Based on these trends in the x_0 curves, the "Macaws" x_0 curve was selected to represent an average normal lightness-class image, Figure 9a.

To summarize, for each of the image lightness-classes x_0 and σ parameter curves were selected to represent average images from that class. For the high lightness-class, the x_0 and σ parameter curves were selected from the "Couple-on-Beach"

image. The x_0 curve that represented the normal lightness-class was taken from the “Macaws” image. The σ parameter curve for the normal lightness-class was made from a composite of the three images in the class. The x_0 and σ parameter curves for the low lightness-class were taken from the “Horse-Race” image. These curves are shown in Figure 9a-b. The resulting sigmoidal remapping functions derived from these parameters are shown in Figure 10a-c.

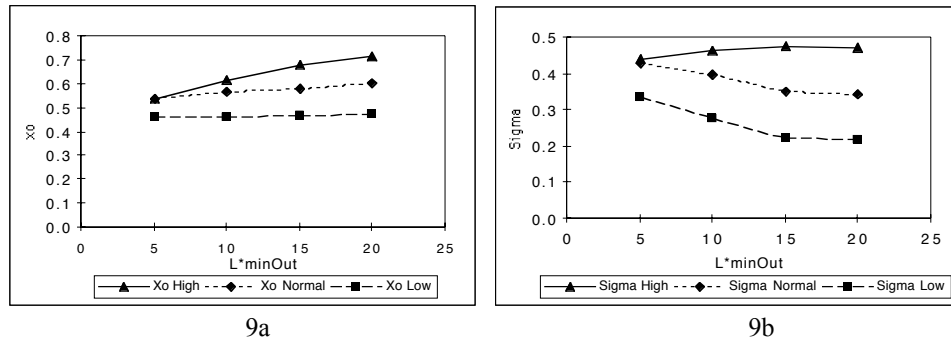


Figure 9a,b Final x_0 and σ parameter curves for the high, normal, and low lightness-classes.

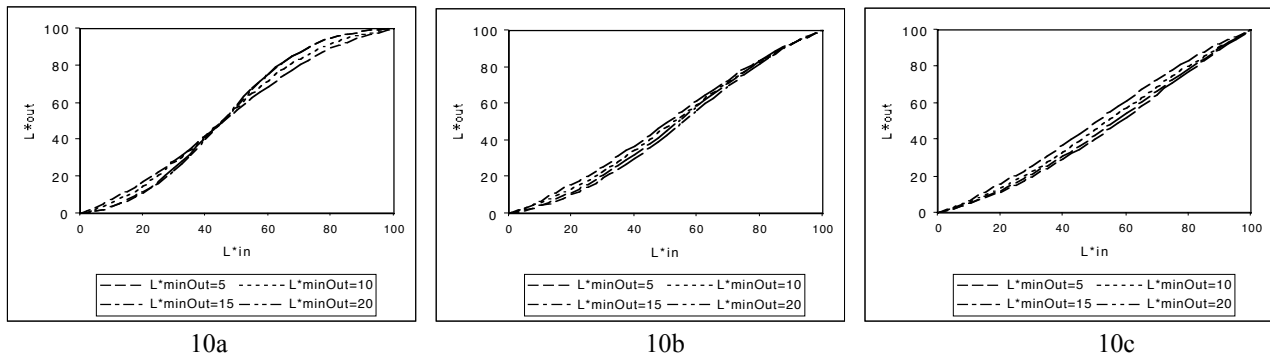


Figure 10a-c Sigmoidal contrast enhancement remapping functions for low (a), normal (b), and high (c) lightness-classes.

6. EMPIRICAL SIGMOID MODEL

Based on the results of Phase 3, it was possible to construct an empirically based model that allows for the automatic selection of x_0 and σ parameters based on the lightness of the 75 percent point of the cumulative lightness histogram. This parameter and the minimum L^* of the output device are used to derive the sigmoidal parameters (x_0 and σ). The x_0 and σ parameters used in this model are given in Table 3 (Appendix). The sigmoidal parameters are selected using a sequential linear interpolation process from the optimal curves generated in Phase 3 (Figure 9a,b).

The sequential interpolation process for x_0 is illustrated in the following steps using the example where the input image has a 75 percent point of its cumulative lightness histogram at $L^*=55$ and an $L^*_{minOut}=18$. The steps involved in the sequential linear interpolation for x_0 are shown in Figure 11 and are given by the following: (Note: σ is calculated in the same manner from the σ parameter curves shown in Figure 9b).

1. Specify the minimum lightness (L^*_{minOut}) of the destination device.
2. Determine the lightness of the 75 percent point of the cumulative histogram for the test image.
3. Determine which parameter curves to use for the interpolation. Compare the lightness of the 75 percent point of the test image to that of the 75 percent points of the reference lightness (high lightness-class = 71 L^* units, normal lightness-class=51 L^* units, and low lightness-class=31 L^* units). If the L^* associated with the 75 percent point of the input cumulative histogram is greater than 71 or less than 31, the high or low lightness-class parameter curves are used respectively.

For example, if the test image has a 75 percent point lightness of $L^*=55$ and an $L^*_{\min\text{Out}}=18$, then this image is bounded on the upper end by the high lightness-class image curve ($L^*=71$) and the lower end by the normal lightness-class image curve ($L^*=51$). As such, subsequent interpolations are performed using these curves as references.

4. Estimate x_o parameters for the test $L^*_{\min\text{Out}}$ level by linearly interpolating between the reference $L^*_{\min\text{Out}}$ levels of $\{5,10,15,20\}$ for the current lightness-class curves.

For the current example, the test $L^*_{\min\text{Out}}$ equals 18. The x_o parameters for the upper and lower bounding lightness-class curves (i.e., $x_{o\text{High}}(18)$ and $x_{o\text{Normal}}(18)$) are estimated at an $L^*_{\min\text{Out}}=18$ from the x_o values at the corresponding $L^*_{\min\text{Out}}$ values of 15 and 20. These relationships are given by:

$$x_{o\text{High}}(18) = \alpha * x_{o\text{High}}(15) + \beta * x_{o\text{High}}(20) \quad (4)$$

$$x_{o\text{Normal}}(18) = \alpha * x_{o\text{Normal}}(15) + \beta * x_{o\text{Normal}}(20) \quad (5)$$

where $x_{o\text{High}}(18)$ and $x_{o\text{Normal}}(18)$ are the estimated x_o values for an $L^*_{\min\text{Out}} = 18$ for the high and normal lightness-classes respectively and $x_{o\text{High}}(15)$, $x_{o\text{High}}(20)$, $x_{o\text{Normal}}(15)$, and $x_{o\text{Normal}}(20)$ are the x_o model values for the high and normal lightness-classes given in Table 3 (Appendix). α and β are the linear interpolation weights given by:

$$\alpha = 1 - \beta \quad (6)$$

$$\beta = \frac{18 - 15}{20 - 15} \quad (7)$$

where the values of 18, 15, and 20 are the corresponding $L^*_{\min\text{Out}}$ values for the x_o parameters used in the interpolation shown in Equations 4 and 5.

5. Estimate final x_o parameter ($x_{o\text{Estimated}}$) for the current image by linearly interpolating between the x_o points estimated in step 4 using the cumulative histogram points for the bounding lightness-classes and that of the current image as weights. The weighting equation used in this calculation is given by:

$$x_{o\text{Estimated}} = \omega_1 * x_{o\text{High}}(18) + \omega_2 * x_{o\text{Normal}}(18) \quad (8)$$

where $x_{o\text{High}}(18)$ and $x_{o\text{Normal}}(18)$ come from Equations 4 and 5. The interpolation parameters ω_1 and ω_2 for this example are given by:

$$\omega_1 = 1 - \omega_2 \quad (9)$$

$$\omega_2 = \frac{55 - 51}{71 - 51} \quad (10)$$

where the values of 55, 51, and 71 are the corresponding lightness values for the 75 percent points of the cumulative lightness histograms for the test image, the normal lightness-class, and the high lightness-class respectively.

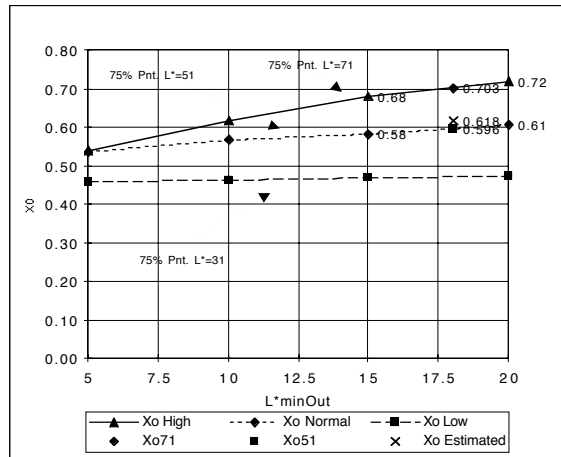


Figure 11. Example interpolation of a x_0 parameter for an input image with its 75 percent point cumulative lightness histogram point at $L^*=55$ and an $L^*_{outMin} = 18$. The “Xo Estimated” point is calculated using linear interpolation between the model parameter points located at L^*_{minOut} values of 15 and 20, using the weighting equations given in Equations 4 and 5.

7. CONCLUSIONS

Based on the results of the experiments performed in this study, it was possible to maintain a large portion, if not all, of the perceived contrast of lightness compressed images by increasing the image contrast using sigmoidal contrast enhancement curves. The form of these enhancement curves was determined based on a simple series of interpolations from a set of optimized reference curves. The only inputs to this process were the lightnesses of the source and destination black points and the lightness corresponding to the 75 percent point of the cumulative lightness histogram of the image. It is believed that these functions will perform a crucial role in developing a more universal approach to color gamut mapping of pictorial images.

ACKNOWLEDGEMENTS

The authors wish to express thanks to the Xerox Corporation and the NSF-NYS/IUCRC and NYSSTF Center for Electronic Imaging Systems for their support.

REFERENCES

1. E.D. Montag and M.D. Fairchild, “Psychophysical Evaluation of Gamut Mapping Techniques Using Simple Rendered Images and Artificial Gamut Boundaries”, *IEEE Trans. Image Proc.*, **6**, pp. 997-989, 1997.
2. J. Morovic and M.R. Luo, “Gamut Mapping Algorithms Based on Psychophysical Experiment”, *Proceedings of the 5th IS&T/SID Color Imaging Conference*, pp. 44-49, 1997.
3. T. Hoshino and R.S. Berns, “Color Gamut Mapping Techniques for Color Hard Copy Images”, *SPIE Proceedings*, **1909**, pp. 152-164, 1993.
4. D.L. MacAdam, “Quality of Color Reproduction”, *Journal of the SMPTE*, **56**, 1951
5. R.S. Berns, R.J. Motta, and M.E. Gorzynski, “CRT Colorimetry. Part 1: Theory and Practice”, *Color Research and Applications*, **18**, pp. 299-314, 1993.
6. G.J. Braun and M.D. Fairchild, “Color Gamut Mapping in a Hue-Linearized CIELAB Color Space”, *Proceedings of the 6th IS&T/SID Color Imaging Conference*, November 1998.
7. C.J. Bartleson and F. Grum, *Optical Radiation Measurements, Vol. 5: Visual Measurements*, Academic Press, 1984.

APPENDIX (Tables)

Table 1. The values in this table represent the number of times a given remapped image was selected as the closest match to the original for the Phase 2 screening process. The highlighted cells indicate the top three sigmoidal remapping functions (S₁-S₉) that were selected the most often. (If two images had the same tally they were both highlighted.) The images corresponding to the highlighted cells were tested in Phase 3.

Image Name	L* _{minOut}	S1	S2	S3	S4	S5	S6	S7	S8	S9
Couple-On-Beach	10	7	5	5	3	8	0	3	3	2
Couple-On-Beach	15	6	2	6	8	5	0	3	1	5
Couple-On-Beach	20	6	2	7	4	7	0	3	2	5
Couple-On-Beach	5	5	4	8	3	6	4	3	2	1
Flower	10	5	2	7	6	6	6	2	0	2
Flower	15	6	2	8	6	4	0	4	1	5
Flower	20	7	4	8	5	5	0	2	1	4
Flower	5	5	5	4	5	5	7	3	1	1
Horse-Race	10	6	4	5	4	2	4	6	2	3
Horse-Race	15	8	7	6	3	1	0	4	3	4
Horse-Race	20	8	4	7	2	3	0	5	4	3
Horse-Race	5	8	5	7	4	1	4	3	2	2
Macaws	10	6	3	6	7	7	0	2	1	4
Macaws	15	5	5	5	7	2	7	2	0	3
Macaws	20	7	4	8	6	3	0	2	1	5
Macaws	5	5	4	5	5	7	5	3	1	1
Raft	10	4	6	5	8	7	2	1	2	1
Raft	15	7	3	5	6	6	5	2	2	0
Raft	20	4	5	7	6	5	4	0	2	3
Raft	5	5	5	4	5	6	5	3	1	2
Temple	10	4	2	7	6	7	1	3	3	3
Temple	15	4	4	6	7	5	5	2	0	3
Temple	20	6	4	7	7	6	0	2	1	3
Temple	5	4	3	3	6	7	8	3	0	2

Table 2. Interval scales from the Phase 3 visual experiment. For each image at each of the four L*_{minOut} levels, the highlighted cell indicates which of the (S₁-S₉) curves produced the best match to the original. Empty cells indicate that the image was not involved in this test.

Image Name	L* _{minOut}	S1	S2	S3	S4	S5	S6	S7	S8	S9
Couple-On-Beach	10	-0.253	0.456	-0.842	-	0.639	-	-	-	-
Couple-On-Beach	15	-0.399	-	0.379	-0.379	-0.637	-	-	-	1.035
Couple-On-Beach	20	-0.132	-	-0.121	-	0.379	-	-	-	-0.126
Couple-On-Beach	5	0.271	-	0.507	-	-0.778	-	-	-	-
Flower	10	-0.652	-	0.006	1.284	-0.640	0.001	-	-	-
Flower	15	-0.379	-	-0.385	0.637	-	-	-	-	0.128
Flower	20	0.397	-	-1.434	0.399	0.639	-	-	-	-
Flower	5	0.289	-0.251	-	0.934	-0.948	-0.024	-	-	-
Horse-Race	10	-0.128	-	0.379	-	-	-	-0.251	-	-
Horse-Race	15	-0.260	0.000	0.260	-	-	-	-	-	-
Horse-Race	20	-0.126	-	0.650	-	-	-	-0.524	-	-
Horse-Race	5	-0.132	-0.507	0.639	-	-	-	-	-	-
Macaws	10	-0.006	-	-0.253	-0.126	0.385	0.000	-	-	-
Macaws	15	-0.251	1.179	0.379	-0.401	-	-0.905	-	-	-
Macaws	20	0.002	-	-0.802	1.053	-	-	-	-	-0.253
Macaws	5	0.385	-	-0.381	0.379	-0.637	0.253	-	-	-
Raft	10	0.399	0.126	-0.260	-0.139	-0.126	-	-	-	-
Raft	15	0.145	-	-0.271	1.101	-0.260	-0.716	-	-	-
Raft	20	-0.859	1.767	-0.276	-0.507	-0.126	-	-	-	-
Raft	5	-0.253	-0.639	-	0.905	-0.399	0.385	-	-	-
Temple	10	-0.128	-	-1.053	-0.018	1.199	-	-	-	-
Temple	15	-0.271	-	-0.500	1.439	-0.421	-0.247	-	-	-
Temple	20	-0.013	-	-0.784	-0.377	1.174	-	-	-	-
Temple	5	-0.132	-	-	-0.385	1.024	-0.507	-	-	-

Table 3. Optimal x₀ and σ parameters for the three image lightness classes and L*_{minOut} levels from Phase 3.

High Lightness-class			Normal Lightness-class			Low Lightness-class		
L* _{minOut}	x ₀	σ	L* _{minOut}	x ₀	σ	L* _{minOut}	x ₀	σ
5	54.0	44.1	5	53.7	43.0	5	46.1	33.6
10	61.7	46.4	10	56.8	40.0	10	46.4	27.7
15	68.0	47.5	15	58.2	35.0	15	46.9	22.4
20	71.9	47.5	20	60.6	34.5	20	47.5	22.0